JOURNAL OF APPLIED PHYSICS VOLUME 88, NUMBER 8 15 OCTOBER 2000

Impedance field and noise of submicrometer n^+nn^+ diodes: Analytical approach

O. M. Bulashenko,[a] P. Gaubert, L. Varani, J. C. Vaissiere, and J. P. Nougier
Centre d'Electronique et de Micro-optoélectronique de Montpellier, Université Montpellier II, place E. Bataillon, 34095 Montpellier cedex 5, France

(Received 8 May 2000; accepted for publication 11 July 2000)

A theoretical model for the noise properties of n^+nn^+ diodes in the drift-diffusion framework is presented. In contrast with previous approaches, our model incorporates both the drift and diffusive parts of the current under inhomogeneous and hot-carrier conditions. Closed analytical expressions describing the transport and noise characteristics of submicrometer n^+nn^+ diodes, in which the diode base (n part) and the contacts (n^+ parts) are coupled in a self-consistent way, are obtained. © *2000 American Institute of Physics.* [S0021-8979(00)06820-1]

I. INTRODUCTION

The noise analysis of submicron semiconductor devices, in which both space-inhomogeneous and hot-carriers conditions may be involved, has recently attracted much attention. In particular, considerable efforts have been devoted to the theoretical investigation of noise in a n^+nn^+ diode, which, on the one hand is the simplest example of a nonhomogeneous semiconductor device and on the other forms the basis for various devices such as field-effect transistors, switchers, photodiodes, etc. The modeling of noise in n^+nn^+ diodes has been recently performed by numerical procedures: the Monte Carlo (MC) method[1,2] and the hydrodynamic (HD) approach.[3,4] While the former is a stochastic technique, which intrinsically includes the microscopic fluctuations, the latter is a deterministic procedure calculating the noise spectral density by means of the impedance field method.[4] The HD approach is a promising tool, since it takes into account all the necessary kinetic information on almost the same grounds as the MC method but, in addition, is able to compute the local impedance and noise distributions, which are of importance to evaluate the device performance. The local quantities are usually computed in two steps. In the first step, the stationary profiles of the transport characteristics (the electric field, electron density, mean velocity, etc.) are calculated. Then, in the second step, the evolution of perturbations around the steady states located in various points of the structure are considered from which the Green function, the impedance field, and the voltage noise spectral density are computed. Within the HD approach the calculation of the evolution of perturbations is a numerical procedure.

Recently, the drift-diffusion (DD) approach has been proposed for the local noise analysis of nonhomogeneous structures.[5,6] Although the DD model is based on the local field approximation, i.e., the kinetic coefficients (mobility, diffusion coefficient) are functions of the local electric field, the system of equations to be solved is simpler, which gives the possibility of avoiding the second step in the calculations. Indeed, in the DD framework the transport equation is reduced to a second-order differential equation with respect to the electric field. This results in the possibility of finding analytical formulas for the Green functions of the linearized operator, and once the steady-state field distribution is found, the local impedance and noise can be immediately obtained by simple integration over the steady-state quantities, without computing numerically the evolution of perturbations throughout the device. The effectiveness of this technique has been demonstrated on various nonhomogeneous structures such as n^+n homojunctions,[5,6] Schottky barrier contacts,[7] and Schottky diodes.[8]

The aim of this article is to apply the DD framework to the local noise analysis of submicron n^+nn^+ diodes and to obtain in a closed analytical form the impedance field and the local noise characteristics. In long diodes ($\gtrsim 1\,\mu$m), the diffusive part of the current may be neglected and only the drift part is usually considered. For that case the analytical formulas for the impedance field in the diode base (the contacts are excluded from the consideration) were calculated many years ago.[9] In submicron diodes, the length of the diode base is on the order of the screening length in the material, and the space-charge near-contact layers extend over the whole sample leading to a strong inhomogeneity of the electron transport. Under these conditions, the diffusion current cannot be neglected. Taking into account both the diffusive and drift current components, we have obtained closed analytical expressions, which describe the transport and noise characteristics of the n^+nn^+ diode, in which the diode base (n part) and the contacts (n^+ parts) are coupled in a self-consistent way. Moreover, the mobility and the diffusion coefficient are considered to be electric-field dependent, so that the hot-carrier regime is also included. The comparison between the drift-diffusion model and the Monte Carlo simulation will be taken as validating proof of the DD model.

The article is organized as follows. In Sec. II the basic equations for the description of transport and fluctuations in n^+nn^+ diodes in the DD framework is described. In Sec. III the steady-state spatial profiles for the electric field, carrier density, and electric potential, as well as the current–voltage

---

[a] Author to whom correspondence should be addressed; present address: Dept. Física Fonamental, Universitat de Barcelona, Av. Diagonal 647, E-08028 Barcelona, Spain; Electronic mail: oleg@ffn.ub.es

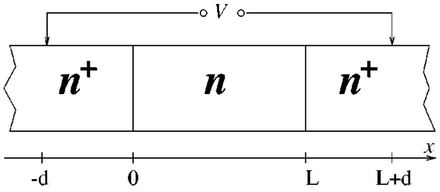

FIG. 1. Geometry of the diode.

(I–V) characteristics are numerically obtained for the particular case of a Si n^+nn^+ diode of different lengths and under different applied voltage biases. The analytical expressions for the impedance and noise characteristics are derived in Sec. IV. These expressions are evaluated by making use of the steady-state profiles obtained in Sec. III. Finally, in Sec. V we sum up the main contributions of the article.

II. DRIFT-DIFFUSION MODEL: TRANSPORT AND FLUCTUATIONS

A. Steady-state transport

Consider an n^+nn^+ diode in which the low-doped diode base n of the length L is sandwiched between two heavily doped contacts n^+ each of the length d (Fig. 1). The doping concentrations in the base and the contacts are N_D^- and N_D^+, respectively.

We are interested in modeling the noise at low frequencies corresponding to the time scale much longer than the dielectric relaxation time. Therefore, the displacement current may be neglected. In the DD approximation, combining the current and Poisson equations, the electric transport in the diode is governed by the second-order differential equation for the steady electric-field profile $E(x)$.[5,6] We write this equation for the n and n^+ regions as

$$D(E)\frac{d^2E}{dx^2}+v(E)\left(\frac{dE}{dx}-\frac{q}{\epsilon}N_D^-\right)=-\frac{I}{\epsilon A},\qquad 0<x<L, \tag{1a}$$

$$\tilde{D}(E)\frac{d^2E}{dx^2}+\tilde{v}(E)\left(\frac{dE}{dx}-\frac{q}{\epsilon}N_D^+\right)=-\frac{I}{\epsilon A},\qquad -d<x<0,\quad L<x<L+d, \tag{1b}$$

where I is the steady-state electric current, q the electron charge, ϵ the dielectric permittivity, A the sample cross-sectional area, $D(E)$ the diffusion coefficient, and $v(E)$ the electron drift velocity. These equations are nonlinear, since the drift velocity $v(E)$ and the diffusion coefficient $D(E)$ depend on the electric field. For the n^+ region we marked them by a tilde to distinguish them from those for the n region.

At the interfaces $x=0$ and $x=L$ from the continuity of the electric field and electron density we obtain the following boundary conditions:

$$E_{0^-}=E_{0^+},\quad E_{L^-}=E_{L^+}, \tag{2a}$$

$$\left.\frac{dE}{dx}\right|_{x=0^+}-\left.\frac{dE}{dx}\right|_{x=0^-}=\frac{q}{\epsilon}(N_D^- - N_D^+), \tag{2b}$$

$$\left.\frac{dE}{dx}\right|_{x=L^+}-\left.\frac{dE}{dx}\right|_{x=L^-}=\frac{q}{\epsilon}(N_D^+ - N_D^-). \tag{2c}$$

Hereafter, we use the subindex 0^- (0^+) when a discontinuous quantity is evaluated at the contact-sample interface at $x=0$ from the left (right). The similar notations (L^- and L^+) are used for the point $x=L$.

Finally, at the ends of the diode the quasineutrality conditions impose

$$\left.\frac{dE}{dx}\right|_{x=-d}=\left.\frac{dE}{dx}\right|_{x=L+d}=0. \tag{3}$$

The contact lengths d are chosen to be large enough, i.e., much larger than the Debye screening length $L_D^+=(\epsilon k_BT/q^2N_D^+)^{1/2}$ to guarantee the quasineutrality conditions.

It should be emphasized that the continuity of both the electric field and electron density at the interfaces [Eqs. (2)] cannot be fulfilled simultaneously if the diffusion current is not taken into account and only the drift component of the current is considered. For the latter case the transport equation is of the first order, and once the electric field is assumed to be continuous, the electron density must have a jump at the interface to fulfill the continuity of the current, which is unphysical. So, if the diffusion current is neglected, it is impossible to couple self-consistently the diode base with the contacts.

B. Fluctuations

The noise properties of the diode may be analyzed by calculating the fluctuations of the electric field along the structure. We assume from the current-driven operation condition, under which the diode is placed in a high-impedance external circuit that the current is maintained constant and the voltage fluctuations are computed. In the Langevin approach, the fluctuations of the electric field δE_x at a slice x satisfy the linearized version of Eqs. (1) with a noise source term for the current δI_x.[5,6]

Consider the n region, $0<x<L$. By linearizing Eq. (1a), one gets a linear nonhomogeneous equation for the electric-field fluctuation δE_x in the form

$$\hat{L}\,\delta E_x=-\delta I_x/(\epsilon A), \tag{4}$$

with the operator $\hat{L}$ given by[6]

$$\hat{L}=D(E)\frac{d^2}{dx^2}+v(E)\frac{d}{dx}+D'(E)\frac{d^2E}{dx^2}+v'(E)\left(\frac{dE}{dx}-\frac{q}{\epsilon}N_D^-\right). \tag{5}$$

Note that $\hat{L}$ is a *second-order* differential operator, in contrast to the previous simpler studies,[9,10] where it was of the first order, since the diffusion has not been included. Here, δI_x represents the stochastic current. When the noise is due mainly to velocity fluctuations of carriers (diffusion noise) and spatial correlations are neglected, it has zero mean and δ-type correlation function $\langle \delta I_x \delta I_{x'} \rangle = AK(x)\Delta f \delta(x-x')$ with[11]

$$K(x)=4q^2 n(x) D(x), \tag{6}$$

with Δf being the frequency bandwidth. For the n^+ parts of the diode, one may write the similar transport equation for the fluctuations $\hat{\tilde{L}}\delta\tilde{E}_x = -\delta\tilde{I}_x/(\epsilon A)$, with the operator $\hat{\tilde{L}}$ given by the formula similar to Eq. (5) (marking the corresponding quantities by a tilde and changing the doping concentration N_D^- to N_D^+).

The boundary conditions for the fluctuations at the n^+n interfaces follow from those for the steady state given by Eq. (2) and the continuity conditions for the fluctuating electric field and electron density

$$\delta E_{0^-} = \delta E_{0^+} \equiv \delta E_0, \tag{7a}$$

$$\delta E_{L^-} = \delta E_{L^+} \equiv \delta E_L, \tag{7b}$$

$$\left. \frac{d\,\delta E_x}{dx} \right|_{x=0^-} = \left. \frac{d\,\delta E_x}{dx} \right|_{x=0^+}, \tag{7c}$$

$$\left. \frac{d\,\delta E_x}{dx} \right|_{x=L^-} = \left. \frac{d\,\delta E_x}{dx} \right|_{x=L^+}. \tag{7d}$$

At the diode ends, we suppose

$$\delta E_{-d} = \delta E_{L+d} = 0, \tag{8}$$

since the contribution to the noise from distances much larger than the Debye length is screened out.

Equations (4)–(8) constitute a complete set of equations to analyze the noise properties of an n^+nn^+ diode in the DD framework.

III. STEADY-STATE SPATIAL PROFILES AND *I–V* PLOTS

To analyze the local and global noise properties of a diode we must first find the stationary spatial profiles. To this purpose, we solve numerically Eqs. (1) with the boundary conditions (2) and (3) by making use of a finite difference scheme. For the field-dependent mobility μ and diffusion coefficient D we use the analytical approximations[12]

$$\mu(E)=\frac{\mu_0}{[1+(E/E_c)^\beta]^{1/\beta}},$$
$$D(E)=\frac{D_0}{[1+(E/E_c)^\beta]^{(\beta-1)/\beta}}, \tag{9}$$

where $E_c = v_s/\mu_0$ is the critical field determined by the saturation drift velocity v_s, μ_0 is the low-field mobility, and β is a dimensionless parameter chosen to give the best possible fit over the entire field range. Below we shall use the following analytical approximations giving a good fit for the data obtained from the MC simulations for n-Si:[12–14]

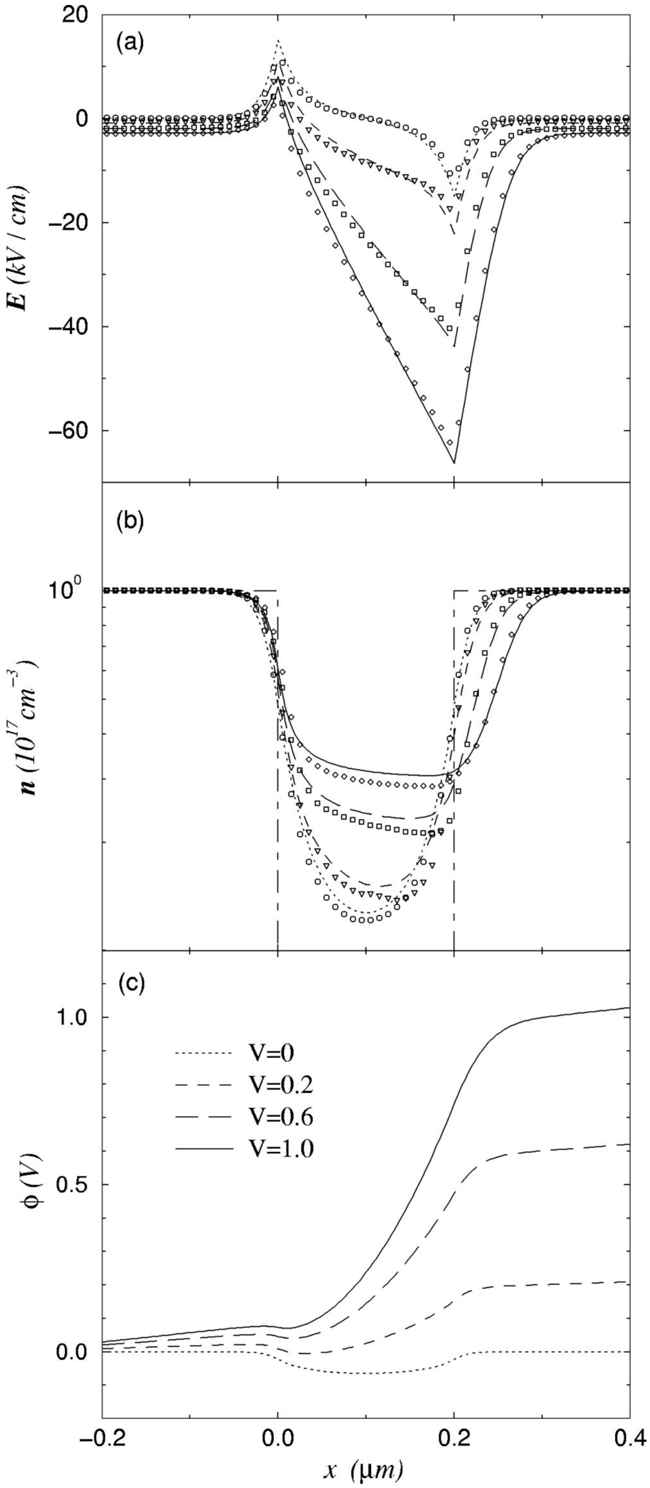

FIG. 2. Stationary profiles for electric field $E(x)$ (a), electron density $n(x)$ (b), and electric potential $\phi(x)$ (c) for n-Si n^+nn^+ diode of length $L=0.2$ μm for different applied voltages V. The Monte Carlo results of Ref. 15 are shown for comparison (symbols).

$$\mu_0(T)=55.24+\frac{7.12\times10^8 T^{-2.3}-55.24}{1+0.177(T/300)^{-3.8}},$$
$$v_s(T)=\frac{2.4\times10^7}{1+0.8(T/600)}, \quad \beta=1.5, \tag{10}$$

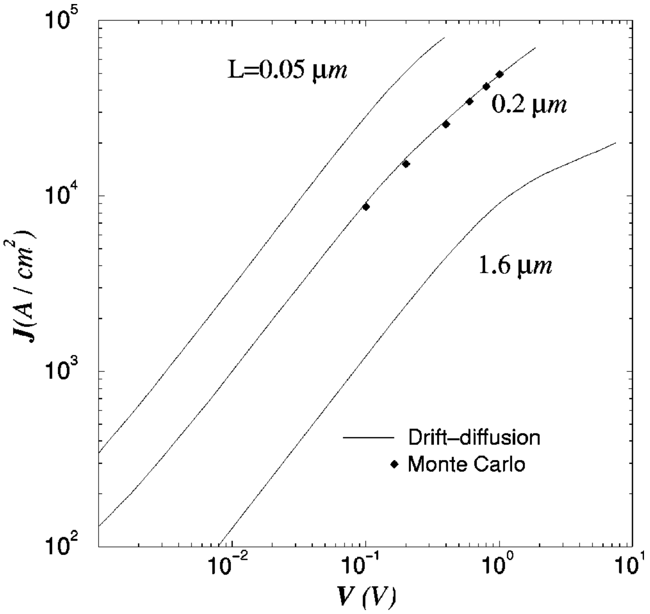

FIG. 3. I–V characteristics for n^+nn^+ diodes of different lengths.

where the lattice temperature T is in K, the saturation velocity is in cm/s, and the mobility is in cm^2/(V s). With the purpose of obtaining the steady-state solutions consistent with the MC results, we consider the same set of parameters used in Ref. 15: the temperature $T=300$ K, the dielectric permittivity $\epsilon=11.8$, the doping concentration in the diode base 10^{16} cm^{-3}, in the n^+ contacts 10^{17} cm^{-3}, the length of the diode base $L=0.2$ μm, and the length of the contacts $d=0.2$ μm (the contacts are sufficiently long to guarantee the quasineutrality conditions at $x=-d$ and $x=L+d$). For this set of parameters we have the screening lengths in the contact and the base $L_D^+\approx 0.013$ μm and $L_D^-\approx 0.04$ μm, respectively.

The stationary electric-field profiles $E(x)$ obtained from the DD model, Eqs. (1)–(3), with the field-dependent coefficients Eq. (9), are shown in Fig. 2(a) for different applied voltage biases V. Since the current I is the input parameter in our model, and the bias $V=\int_{-d}^{L+d}E(x)dx$ is the result, in order to make a comparison with the MC simulations, in which the bias is the input parameter, we make iterations by changing the current until the desired bias V is achieved. The results are seen to be reasonably close to those obtained from the MC simulations.[15] The electron density $n(x)$ found from the field profiles is also in a good agreement [Fig. 2(b)]. It is seen that the charge is redistributed near the interfaces to equilibrate the Fermi levels of the regions with different doping, forming dipole layers with a positive charge at the n^+ side, and a negative charge at the n side [Fig. 2(b)]. The dipoles produce two spikes of the electric field at the contacts [Fig. 2(a)], which extend over several Debye lengths L_D^+ into the n^+ regions and several L_D^- into the n region. These spikes produce a voltage drop (built-in voltage) between the contacts and the diode base, which gives rise to the formation of the potential minimum when the bias is applied [see Fig. 2(c) for the potential profile $\phi(x)=\int_0^x E(x')dx'$].

A comparison of the I–V characteristics for the structures of different lengths L is shown in Fig. 3. At low biases the I–V curves are linear for any L. At high biases the characteristics become sublinear due to the hot-electrons effect. This effect is pronounced for long diodes ($L=1.6$ μm), whereas for submicrometer diodes the deviation from the linear dependence is not large in the range of voltages investigated. The results for $L=0.2$ μm are in excellent agreement with the MC simulations.[15]

We have also studied how the spatial profiles are changed when the diode length L is scaled down, while the length of the contacts d is fixed. The results for the same current density $J=2\times 10^4$ A/cm^2 are shown in Fig. 4. It is clearly seen from Fig. 4(a), where the electric-field distributions are plotted, why the hot-electron effects are not pronounced in submicrometer diodes. The spillover effect is also important for short diodes [see Fig. 4(b)].

IV. IMPEDANCE AND NOISE

To characterize the noise properties of an n^+nn^+ diode, we have to solve a second-order stochastic differential Equation (4) with the differential operator Eq. (5) containing space dependent coefficients [this space dependence comes through the space dependence of the electric field $E(x)$]. The general scheme to solve this equation analytically has been outlined in Ref. 6. We write the solution for the n part of the diode in the form

$$\delta E_x=\rho(x)\int_{C_1}^{x}\frac{u(\xi)}{\epsilon AD(\xi)W(\xi)}\,\delta I_\xi\,d\xi - u(x)\int_{C_2}^{x}\frac{\rho(\xi)}{\epsilon AD(\xi)W(\xi)}\,\delta I_\xi\,d\xi, \tag{11}$$

where $\rho(x)=dE/dx$ and $u(x)=\rho(x)\int_C^x W(x')/\rho^2(x')dx'$ are the solutions of the homogeneous equation corresponding to Eq. (4), and $W(x)=\rho(x)u'(x)-u(x)\rho'(x)$ is the Wronskian. The similar solutions may be written for the contacts, with the functions $\tilde{v}$, $\tilde{D}$, $\tilde{W}$, and $\tilde{u}$ marked by a tilde. Then, the integration constants can be determined from the boundary conditions, Eqs. (7) and (8), at the interfaces and at the ends of the diode. The solution for each part of the diode becomes

$$\delta\tilde{E}_x=-\rho(x)\int_{x}^{0}\frac{\tilde{u}(\xi)}{\tilde{\Psi}(\xi)}\,\delta I_\xi\,d\xi-\tilde{u}(x)\int_{-d}^{x}\frac{\rho(\xi)}{\tilde{\Psi}(\xi)}\,\delta I_\xi\,d\xi + \delta E_0\frac{\rho(x)}{\rho_{0^-}}, \quad -d<x<0, \tag{12a}$$

$$\delta E_x=\rho(x)\int_{0}^{x}\frac{u(\xi)}{\Psi(\xi)}\,\delta I_\xi\,d\xi+u(x)\int_{x}^{L}\frac{\rho(\xi)}{\Psi(\xi)}\,\delta I_\xi\,d\xi + \delta E_0\frac{\rho(x)}{\rho_{0^+}}+\gamma u(x), \quad 0<x<L, \tag{12b}$$

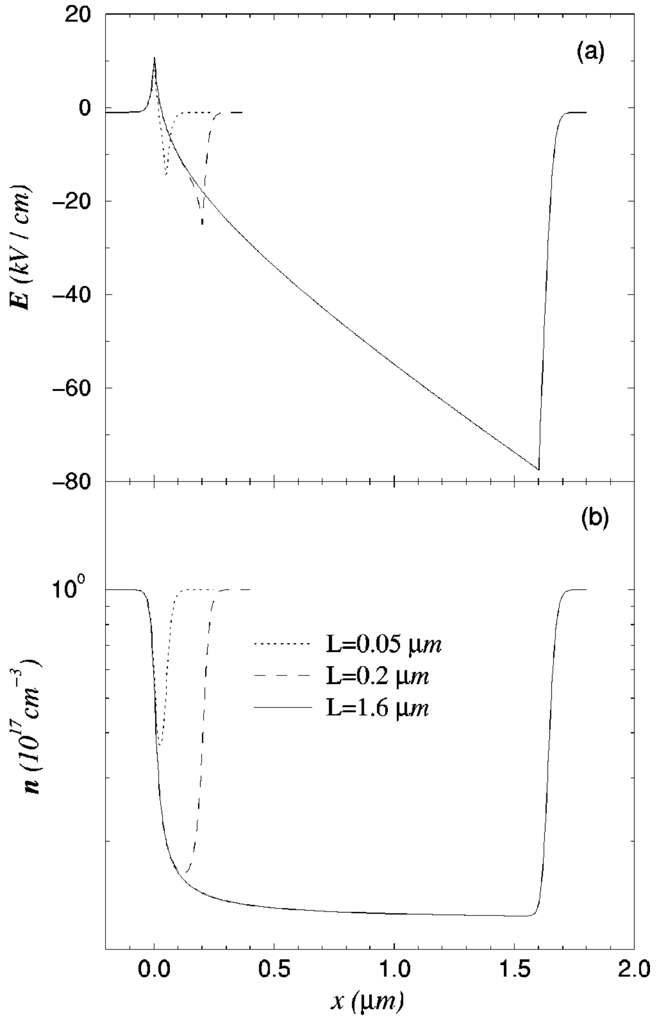

FIG. 4. Stationary profiles for electric field $E(x)$ (a) and electron density $n(x)$ (b) for n^+nn^+ diodes of different lengths L for the same current density $J=2\times10^4$ A/cm^2.

$$\delta\tilde{E}_x=\rho(x)\int_L^x\frac{\tilde{u}(\xi)}{\tilde{\Psi}(\xi)}\,\delta I_\xi\,d\xi+\tilde{u}(x)\int_x^{L+d}\frac{\rho(\xi)}{\tilde{\Psi}(\xi)}\,\delta I_\xi\,d\xi$$

$$+\,\delta E_L\frac{\rho(x)}{\rho_{L^+}},\quad L<x<L+d, \tag{12c}$$

where $\Psi(x)=\epsilon AD(x)W(x)$, $\tilde{\Psi}(x)=\epsilon A\tilde{D}(x)\tilde{W}(x)$, $W(x)=\exp\{-\int_0^x v[E(\xi)]/D[E(\xi)]d\xi\}$, $\tilde{W}(x)=\exp\{-\int_{\tilde{C}}^x\tilde{v}[E(\xi)]/\tilde{D}[E(\xi)]d\xi\}$ with $\tilde{C}=0$, for $-d<x<0$, and $\tilde{C}=L$ for $L<x<L+d$, and we have imposed $\tilde{u}(0^-)=u(0^+)=\tilde{u}(L^+)=0$ (the boundary conditions for the auxiliary functions u and $\tilde{u}$ do not affect the results[6]). Thus, we have three unknowns: δE_0, δE_L, and γ, and in order to find them we use three conditions: Eqs. (7b), (7c), and (7d). We find

$$\gamma=\frac{1}{\Delta}\left(-\frac{\delta E_0^*}{\rho_{0^+}}+\frac{\delta E_L^*}{\rho_{L^-}}-\delta X\right),$$

$$\delta E_0=\delta E_0^*\left(1-\frac{\rho^\star}{\rho_{0^+}}\right)+\delta E_L^*\frac{\rho^\star}{\rho_{L^-}}-\rho^\star\,\delta X,$$

$$\delta E_L=\delta E_0^*\frac{\overline{\rho^\star}}{\rho_{0^+}}+\delta E_L^*\left(1-\frac{\overline{\rho^\star}}{\rho_{L^-}}\right)+\overline{\rho^\star}\,\delta X,$$

where we have denoted

$$\delta E_0^*=\frac{L_n\tilde{W}_0}{\rho_{0^-}W_0}\int_{-d}^{0}\frac{\rho(\xi)}{\tilde{\Psi}(\xi)}\,\delta I_\xi\,d\xi+\frac{L_n}{\rho_{0^+}}\int_0^L\frac{\rho(\xi)}{\Psi(\xi)}\,\delta I_\xi\,d\xi,$$

$$\delta E_L^*=\frac{\overline{L_n}\tilde{W}_L}{\rho_{L^+}W_L}\int_L^{L+d}\frac{\rho(\xi)}{\tilde{\Psi}(\xi)}\,\delta I_\xi\,d\xi,$$

$$\delta X=\int_0^L\frac{u(\xi)}{\Psi(\xi)}\,\delta I_\xi\,d\xi,$$

$$\rho^\star=\frac{L_n}{\rho_{0^+}\Delta},\quad L_n=W_0\left[\frac{\rho'_{0^-}}{\rho_{0^-}}-\frac{\rho'_{0^+}}{\rho_{0^+}}\right]^{-1},$$

$$\overline{\rho^\star}=\frac{\overline{L_n}}{\rho_{L^-}\Delta},\quad \overline{L_n}=W_L\left[\frac{\rho'_{L^-}}{\rho_{L^-}}-\frac{\rho'_{L^+}}{\rho_{L^+}}\right]^{-1},$$

$$\Delta=\frac{L_n}{\rho_{0^+}^2}+\frac{\overline{L_n}}{\rho_{L^-}^2}+\int_0^L\frac{W(\xi)}{\rho^2(\xi)}d\xi,$$

$$\rho_{0^\pm}=\frac{q}{\epsilon}(N_D^{\mp}-n_0),\quad \rho_{L^\pm}=\frac{q}{\epsilon}(N_D^{\pm}-n_L).$$

In the last equations n_0 and n_L are the steady-state electron densities at the interfaces. It is seen from Eqs. (12), that the fluctuating field in our approach is globally coupled throughout the diode and the correlation effects between the diode base (n region) and the contacts (n^+ regions) are included. Apart from allowing us to derive explicit expressions for the impedance field and voltage fluctuations (see below), Eqs. (12) may be used to evaluate the spatial correlations of the electric-field fluctuations $\langle\delta E_x\delta E_{x'}\rangle$ between two different points, between the sample and the contact, between the contacts, etc., under nonhomogeneous transport conditions. These correlations are active over the characteristic screening length of the system.[5]

The fluctuation of the terminal voltage is found as the sum of the voltage fluctuations on the connected in series regions (see Fig. 1) $\delta V=\delta V_{n_1^+}+\delta V_n+\delta V_{n_2^+}=\int_{-d}^0\delta\tilde{E}_x\,dx+\int_0^L\delta E_x\,dx+\int_L^{L+d}\delta\tilde{E}_x\,dx$. Substituting the expressions for the electric-field fluctuations and changing the order of integration, we get

$$\delta V=\int_{-d}^{0}\nabla Z_{n_1^+}^b(x)\,\delta I_x\,dx+\int_0^L\nabla Z_n^b(x)\,\delta I_x\,dx$$

$$+\int_L^{L+d}\nabla Z_{n_2^+}^b(x)\,\delta I_x\,dx+L_{E_\Delta}\delta E_0^*+\overline{L}_{E_\Delta}\delta E_L^*$$

$$+(E_\Delta-E_L)\,\delta X, \tag{13}$$

where

$$\nabla Z^b_{n_1^+}(x) = -\frac{\tilde{u}(x)}{\tilde{\Psi}(x)}\int_{-d}^{x}\rho(\xi)d\xi - \frac{\rho(x)}{\tilde{\Psi}(x)}\int_{x}^{0}\tilde{u}(\xi)d\xi,$$

$$\nabla Z^b_{n}(x) = \frac{u(x)}{\Psi(x)}\int_{x}^{L}\rho(\xi)d\xi + \frac{\rho(x)}{\Psi(x)}\int_{0}^{x}u(\xi)d\xi, \qquad (14)$$

$$\nabla Z^b_{n_2^+}(x) = \frac{\tilde{u}(x)}{\tilde{\Psi}(x)}\int_{x}^{L+d}\rho(\xi)d\xi + \frac{\rho(x)}{\tilde{\Psi}(x)}\int_{L}^{x}\tilde{u}(\xi)d\xi,$$

are the bulk impedance fields corresponding to each ''decoupled'' region, and the characteristic length constants are determined by

$$L_{E_\Delta} = L_E^* + \frac{E_\Delta}{\rho_{0^+}}, \quad \overline{L_{E_\Delta}} = \overline{L_E^*} - \frac{E_\Delta}{\rho_{L^-}},$$

$$L_E^* = E_0\left(\frac{1}{\rho_{0^-}} - \frac{1}{\rho_{0^+}}\right) - \frac{E_{-d}}{\rho_{0^-}},$$

$$\overline{L_E^*} = E_L\left(\frac{1}{\rho_{L^-}} - \frac{1}{\rho_{L^+}}\right) + \frac{E_{L+d}}{\rho_{L^+}}.$$

The parameter

$$E_\Delta = \frac{1}{\Delta}\left(\frac{\overline{L_n}\,\overline{L_E^*}}{\rho_{L^-}} - \frac{L_n L_E^*}{\rho_{0^+}} + \int_0^L \frac{E(x)W(x)}{\rho^2(x)}dx\right) \qquad (15)$$

has a meaning of the characteristic ''coupling'' electric field. It appears due to the long-range Coulomb interaction on the length L of the diode base that is comparable with the screening length. As long as $L \gg L_D^-$, $E_\Delta \to 0$, and the two n^+n junctions may be viewed as decoupled.

Combining in Eq. (13) the terms corresponding to the noise sources located in the same region, we obtain the impedance field of the n^+nn^+ diode as

$$\nabla Z_{\mathrm{diode}}(x) = \nabla Z_{n_1^+}(x) + \nabla Z_n(x) + \nabla Z_{n_2^+}(x), \qquad (16)$$

with

$$\nabla Z_{n_1^+}(x) = \frac{\rho(x)}{\tilde{\Psi}(x)}\left[\beta_1 + \int_x^0 [E(\xi) - E_{-d}]\frac{\tilde{W}(\xi)}{\rho^2(\xi)}d\xi\right],$$

$$\nabla Z_{n}(x) = \frac{\rho(x)}{\Psi(x)}\left[\beta_n + \int_0^x [E_\Delta - E(\xi)]\frac{W(\xi)}{\rho^2(\xi)}d\xi\right], \qquad (17)$$

$$\nabla Z_{n_2^+}(x) = \frac{\rho(x)}{\tilde{\Psi}(x)}\left[\beta_2 + \int_L^x [E_{L+d} - E(\xi)]\frac{\tilde{W}(\xi)}{\rho^2(\xi)}d\xi\right],$$

$$\beta_1 = \frac{L_n L_{E_\Delta}\tilde{W}_0}{\rho_{0^-}W_0}, \quad \beta_n = \frac{L_n L_{E_\Delta}}{\rho_{0^+}}, \quad \beta_2 = \frac{\overline{L_n}\,\overline{L_{E_\Delta}}\tilde{W}_L}{\rho_{L^+}W_L}.$$

Having found $\nabla Z_{\mathrm{diode}}(x)$, one can obtain the spectral density of the voltage fluctuations on the diode as

$$S_V = A\int_{-d}^{L+d}[\nabla Z_{\mathrm{diode}}(x)]^2 K(x)dx. \qquad (18)$$

Thus, the spectral density of the voltage fluctuations is completely expressed through the steady-state quantities, provided the noise sources $K(x)$ are known. Note that the obtained formulas Eqs. (16)–(18) are valid not only for the case of the diffusion noise sources given by Eq. (6), but for the more general case, when other noise sources (e.g., generation–recombination noise) are essential. In this case, the corresponding expressions for $K(x)$ should be used in Eq. (18). The final expression Eq. (18) clearly distinguishes the origin of fluctuations, represented by the local source $K(x)$ from their transmission toward the terminals (where the fluctuations are measured) described by the impedance field $\nabla Z_{\mathrm{diode}}(x)$. It should be noted that the latter is determined by the particular form of the differential operators, which are the operators $\overline{L}$ and $\tilde{\overline{L}}$ in our case of the DD model. Such consideration is very useful in order to characterize the local contribution of different space regions to the net noise, by introducing the quantity $s_V(x)$, such that $S_V = A\int_{-d}^{L+d}s_V(x)dx$.

By using the Poisson equation, the fluctuation of the carrier density δn_x at the point x can be expressed through that for the electric field $\delta n_x = -(\epsilon/q)[d(\delta E_x)/dx]$. Then the spatial correlator $\langle \delta n_x \delta n_{x'} \rangle$ can also be computed. Note

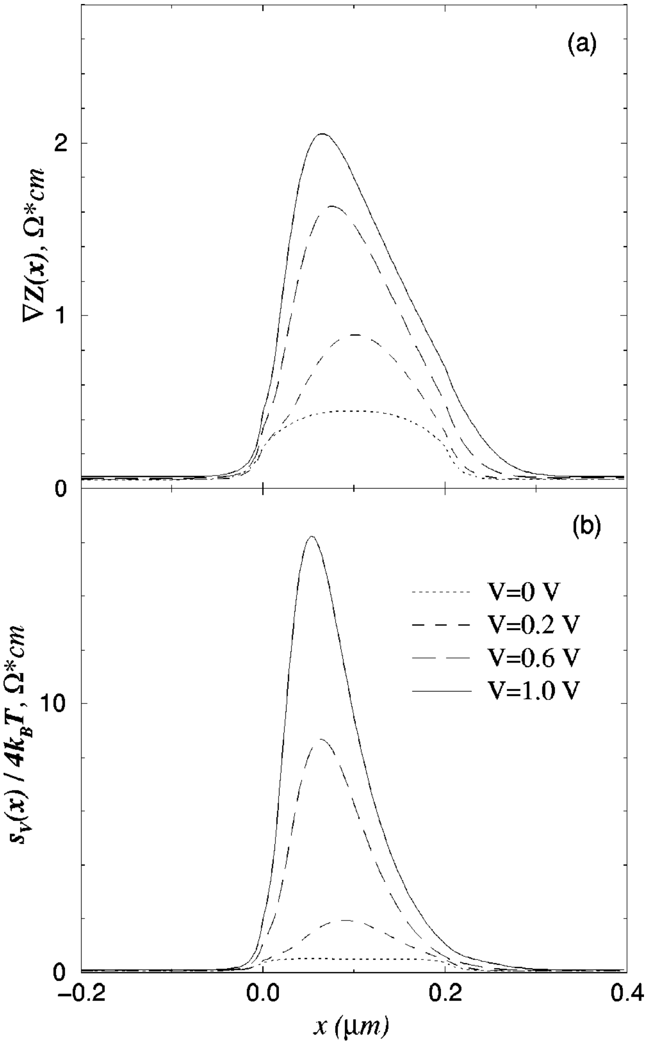

FIG. 5. Spatial profiles for impedance field $\nabla Z(x)$ (a) and local noise distribution $s_V(x)$ (b) for different voltages V obtained from the steady-state distributions of Fig. 2.

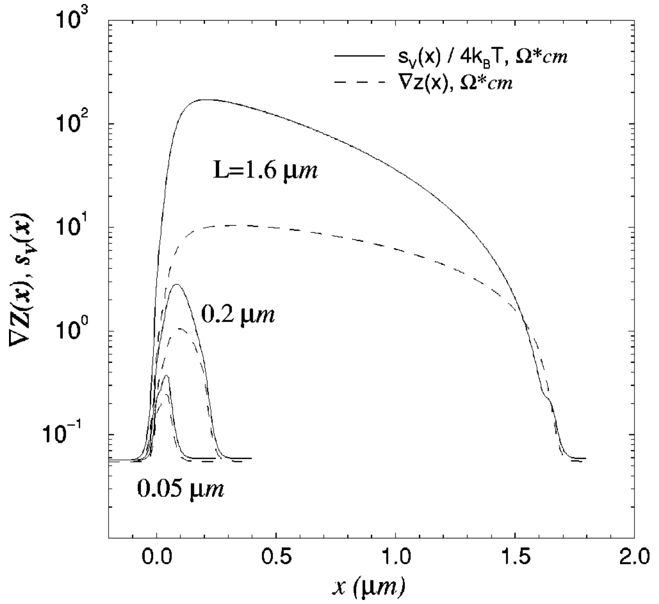

FIG. 6. Spatial profiles for the local impedance field $\nabla Z(x)$ and noise $s_V(x)$ for n^+nn^+ diodes of different lengths L obtained from the steady-state distributions of Fig. 4.

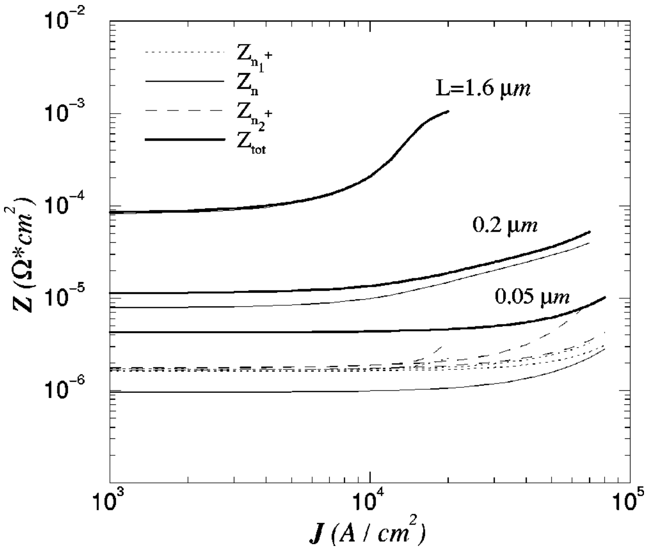

FIG. 7. Impedance Z vs current density J for different diode lengths L. The relative contributions from the contacts and from the diode base are compared.

that the fluctuations of the total number of carriers in different parts of the diode are: $\delta N_n=\int_0^L\delta n_x\,dx=(\epsilon/q)(\delta E_0-\delta E_L)$, $\delta N_{n_1^+}=\int_{-d}^0\delta\tilde{n}_x\,dx=-(\epsilon/q)\delta E_0$, and $\delta N_{n_2^+}=\int_L^{L+d}\delta\tilde{n}_x\,dx=(\epsilon/q)\delta E_L$. Their sum vanishes, $\delta N_{n_1^+}+\delta N_n+\delta N_{n_2^+}=0$ in accordance with a conservation of the total number of particles and the total charge.

The spatial profiles for the impedance field $\nabla Z(x)$ and the local voltage noise $s_V(x)$ for different biases V obtained from the steady-state distributions of Fig. 2 are shown in Fig. 5. At high biases the distributions become asymmetrical with the maximum displaced toward the injecting contact for both the impedance field and noise. At the receiving contact the noise is lower, but it penetrates much deeper inside the contact in comparison with the same effect for the injecting contact. As the device length is scaled down, the magnitude of the local impedance and noise decreases, while the spatial profiles become more symmetrical, which is seen from Fig. 6.

The total impedance Z and the voltage terminal noise S_V are found by integrating the corresponding spatial profiles along the device. The relative contributions of different parts of the diode (the diode base n and the contacts n^+) are shown in Figs. 7 and 8 for different diode lengths L and different current densities $J=I/A$. For all the contributions the behavior is similar: they are constant at low currents (biases) and increasing functions at high currents. The relative contribution however differs for long and short diodes. For the 1.6 μm diode the noise and the impedance of the diode base dominate and the contribution of the contacts is negligible, whereas for submicrometer diodes the contribution from the contacts becomes appreciable. For the 0.2 μm diode this is seen for low and moderate currents, while for the 0.05 μm diode the contact contributions even dominate in almost the entire current range. The latter is due to the fact that the contacts (0.2 μm) are longer than the diode base (0.05 μm).

The noise temperature T_n, estimated from $4k_BT_n=S_V/Z$, is shown in Fig. 9. It is seen that, as the diode length is scaled down, the noise temperature maintains its equilibrium value to much higher currents, which is of importance from the point of view of applications.

V. SUMMARY

In this work we have presented the analytical procedure to compute the local impedance and noise distributions in submicrometer n^+nn^+ diodes, which are characterized by highly inhomogeneous electron transport conditions, for which both the drift and diffusive current components are relevant.

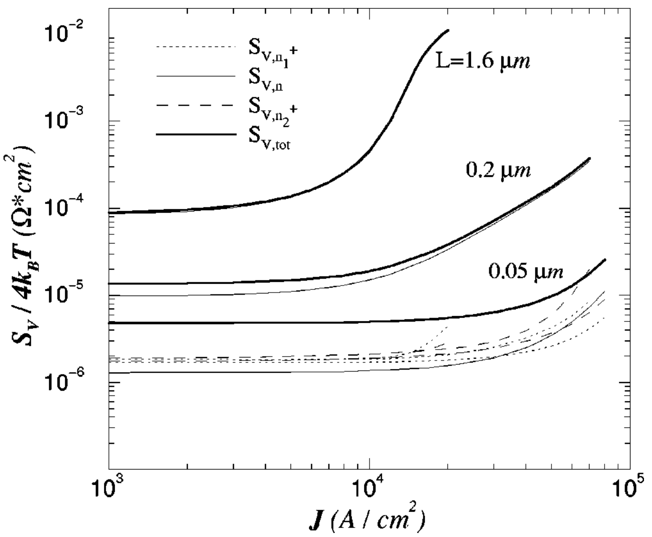

FIG. 8. Voltage fluctuations S_V vs current density J for different diode lengths L. The relative contributions from the contacts and from the diode base are compared.

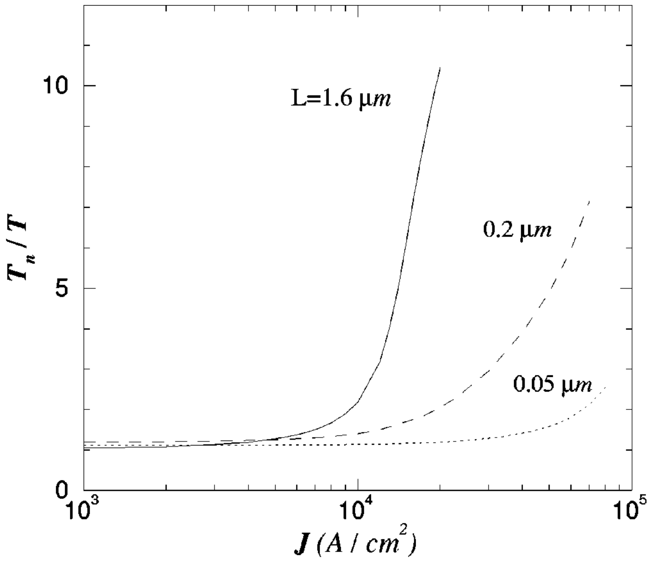

FIG. 9. Noise temperature T_n vs current density J for different diode lengths L.

Our method allows one to solve analytically the second-order differential equation for the field fluctuations throughout the diode in such a way that the contacts are taken into account self-consistently for any applied bias.

We would like to emphasize, that including the diffusion current into consideration allows one to analyze the noise properties of highly inhomogeneous systems, where accumulation and/or depletion layers are present. The present technique is quite universal. Even at strong electric fields, when the standard DD model is no longer valid, one can use the augmented DD model[16] to take into account some of the nonlocal effects, e.g., the drift-velocity overshoot. The resultant equation is again of the second order, and the fluctuation problem may be solved in a way similar to that described in this article. Therefore, our technique can be incorporated into any device model based on the DD approach and its modifications,[16] for which the spatial distributions of the electric field and the carrier concentration are strongly nonuniform.

ACKNOWLEDGMENTS

The authors are grateful to T. González for providing them with the data of the Monte Carlo simulations of Ref. 15. They acknowledge the support by the Ministère de l'Éducation Nationale, de la Recherche et de la Technologie, France through Grant No. DRB4/MDL/n. 99-30.

[1] L. Varani, T. Kuhn, L. Reggiani, and Y. Perlès, Solid-State Electron. **36**, 251 (1993).
[2] E. Starikov, P. Shikhtorov, V. Gružinskis, L. Varani, J. C. Vaissiere, J. P. Nougier, and L. Reggiani, J. Appl. Phys. **79**, 242 (1996).
[3] E. Starikov, P. Shikhtorov, V. Gružinskis, T. González, M. J. Martín, D. Pardo, L. Reggiani, and L. Varani, Semicond. Sci. Technol. **11**, 865 (1996).
[4] E. Starikov *et al.*, J. Appl. Phys. **83**, 2052 (1998).
[5] O. M. Bulashenko, G. Gomila, J. M. Rubí, and V. A. Kochelap, Appl. Phys. Lett. **70**, 3248 (1997).
[6] O. M. Bulashenko, G. Gomila, J. M. Rubí, and V. A. Kochelap, J. Appl. Phys. **83**, 2610 (1998).
[7] G. Gomila, O. M. Bulashenko, and J. M. Rubí, J. Appl. Phys. **83**, 2619 (1998).
[8] G. Gomila and O. M. Bulashenko, J. Appl. Phys. **86**, 1004 (1999).
[9] K. M. van Vliet, A. Friedmann, R. J. J. Zijlstra, A. Gisolf, and A. van der Ziel, J. Appl. Phys. **46**, 1814 (1975).
[10] J. P. Nougier, in *III–V Microelectronics*, edited by J. P. Nougier (Elsevier, Amsterdam, 1991), p. 183.
[11] C. M. van Vliet, IEEE Trans. Electron Devices **41**, 1902 (1994).
[12] M. Ali Omar and L. Reggiani, Solid-State Electron. **30**, 693 (1987).
[13] C. Jacoboni, C. Canali, G. Ottaviani, and A. A. Quaranta, Solid-State Electron. **20**, 77 (1977).
[14] S. Selberherr, Microelectron. Reliab. **24**, 225 (1984).
[15] T. González, PhD thesis, University of Salamanca, 1994.
[16] P. J. Price, J. Appl. Phys. **63**, 4718 (1988).